Catalysis Science and Technology

Supporting Information

Immobilized Grubbs Catalysts on Mesoporous Silica Materials: Insight into Support Characteristics and Their Impact on Catalytic Activity and Product Selectivity

Annelies Dewaele[a], Boris Van Berlo[a], Jan Dijkmans[a], Pierre Jacobs[a], Bert F. Sels[a]*.

[a]Center for Surface Science and Catalysis, KU Leuven, Celestijnenlaan 200F, 3001 Heverlee, Belgium.
*E-mail: Bert.Sels@biw.kuleuven.be

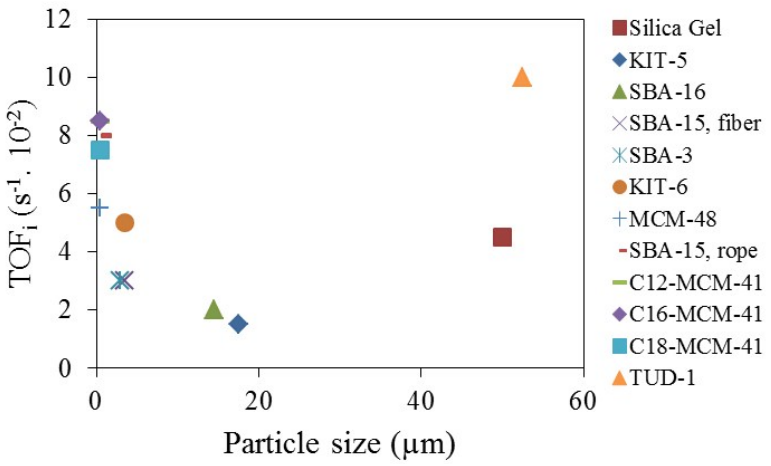

Figure S1. Correlation plot between the initial activity (TOF_i) in the metathesis of cyclooctene of different mesoporous silica and their corresponding particle size.

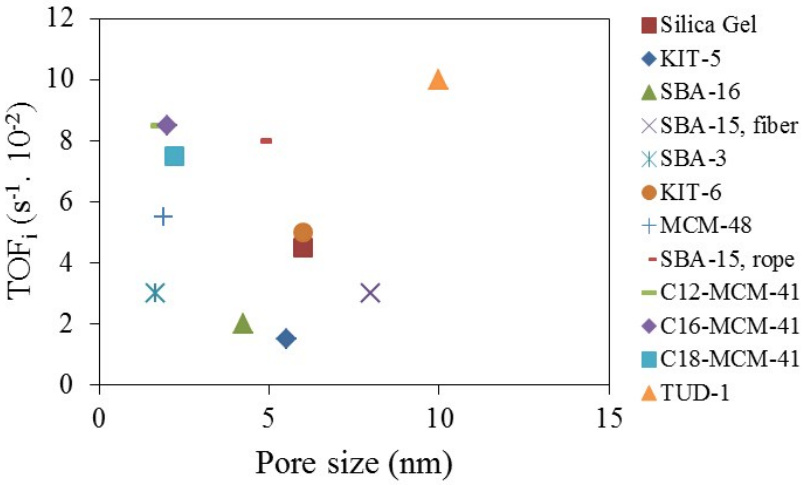

Figure S2. Correlation plot between the initial activity (TOF_i) in the ROMP of cyclooctene of different mesoporous silica and their corresponding pore size.

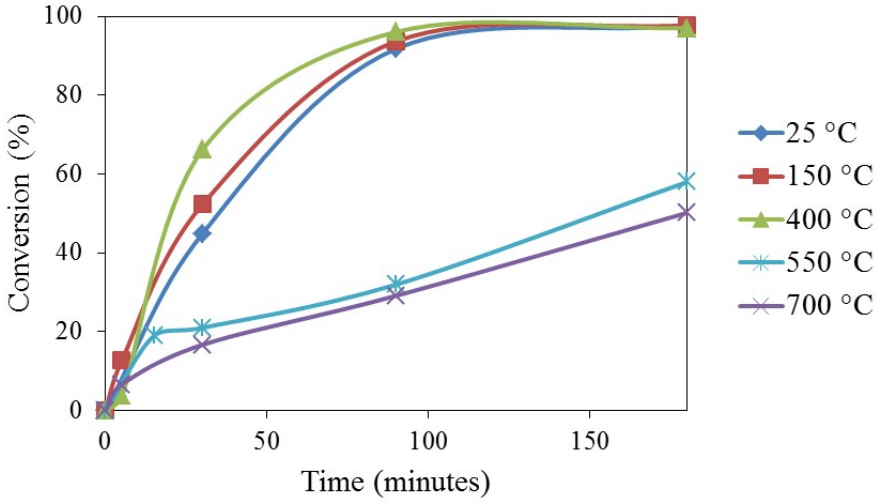

Figure S3. Influence of a thermal treatment of TUD-1 (prior to immobilization of HG 2) on the conversion of cyclooctene with HG2/TUD-1 (0.21 wt%). Reaction conditions: 0.05 M cyclooctene; 5 mL hexane; 50 mg HG 2/TUD-1; 35 °C.

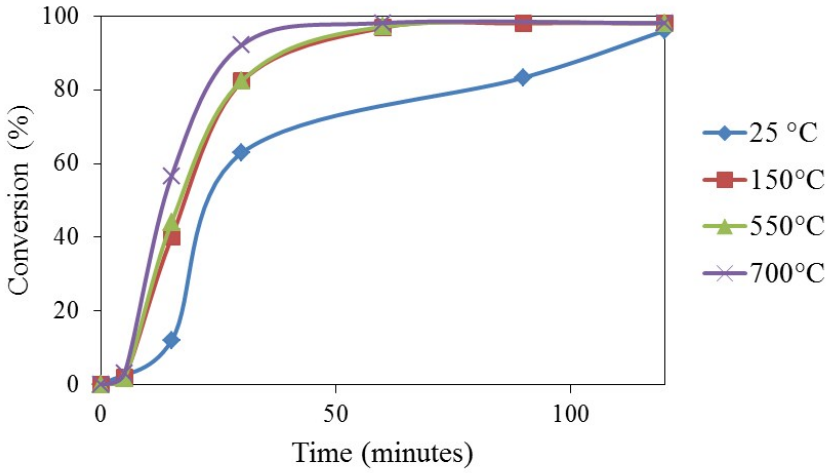

Figure S4. Influence of a thermal treatment of MCM-41 (prior to immobilization of HG 2) on the conversion of cyclooctene with HG2/MCM-41 (0.30 wt%). Reaction conditions: 0.05 M cyclooctene; 5 mL hexane; 50 mg HG 2/MCM-41; 35 °C.

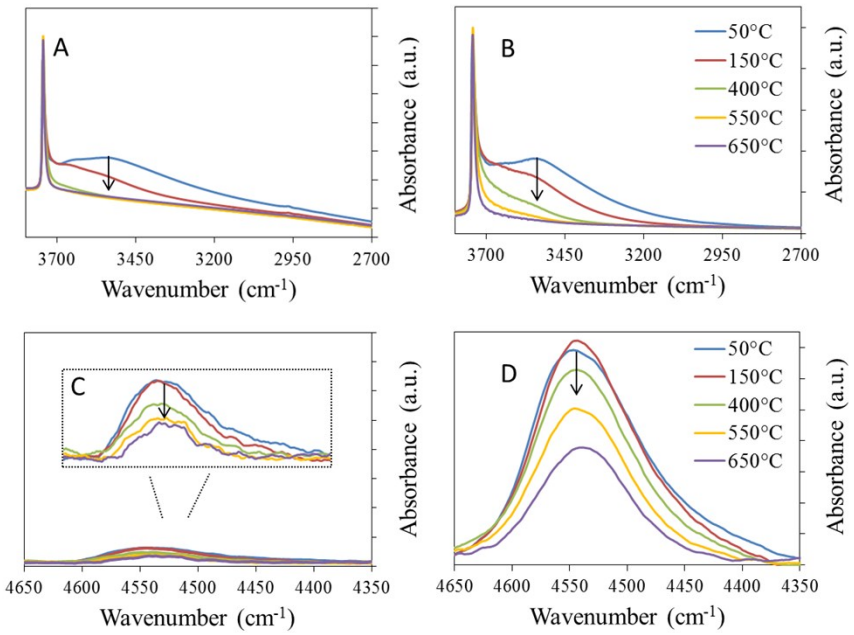

Figure S5. Infrared spectra (ν_{O-H} range) of (A) TUD-1 and (B) MCM-41 and (($\nu+\delta$) $_{O-H}$ range) of (C) TUD-1 and (D) MCM-41 after treatment at different temperatures. Bands at 3520, 3670, 3710 and 3745 cm^{-1} are attributed to H-bonded, internal, terminal and isolated silanols[1], respectively. Even though there are some uncertainties or discrepancies in assignment of the band at 4550 cm^{-1}, many authors are congenial in attributing this band to the combination of $\delta_{(Si-O-H)}$ and $\nu_{(SiO-H)}$.[2-4] For TUD-1, 450°C seems sufficient to form isolated silanols, whereas MCM-41 requires 650°C.

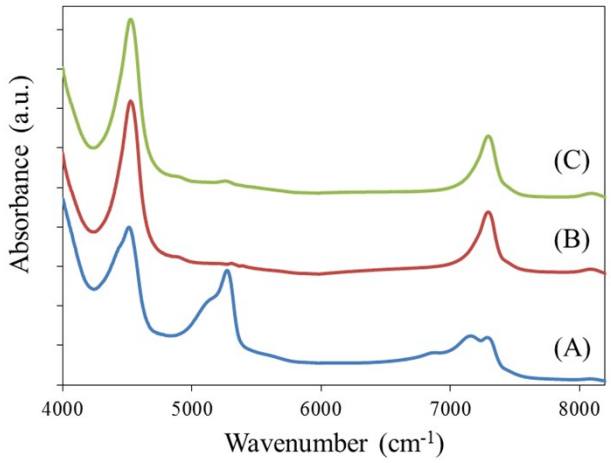

Figure S6. Near-infrared Diffuse Reflectance spectra of (A) untreated MCM-41, (B) MCM-41 dried at 150 °C (atmospheric pressure) and (C) MCM-41 dried at 50 °C under vacuum (10 mbar).

The untreated MCM-41 (A) shows vibrational absorption bands at 5270 and 5119 cm^{-1}, assigned to water molecules hydrogen bonded to vicinal silanol groups and isolated solanol groups respectively. This signal vanishes with samples B and C. The region of 7225-6860 cm^{-1} in sample A is related to silanol groups hydrogen bonded to water molecules, water molecules bonded to silanol groups and hydrogen bonded to other water molecules. The dried samples display the overtone of OH-stretchings of isolated silanols at 7316 cm^{-1} instead. Between 4400 and 4500 cm^{-1} a combination band of silanol OH stretching (hydrogen bonded to water) and siloxane bending appears. The surfaces of samples B and C are chemically identical.

Nitrogen Physisorption measurements

Table S1. Characteristics of TUD-1 and MCM-41 after treatment at 400 and 700 °C.

	$D_{mesopore}$ (nm)	V_{meso} ($cm^3\ g^{-1}$)	BET ($m^2\ g^{-1}$)
TUD-1 (parent)	8-15	1.1	417
TUD-1 (400 °C)	8-15	1.1	380
TUD-1 (700 °C)	8-15	1	360
MCM-41 (parent)	3.3	0.67	1333
MCM-41 (700 °C)	3.3	0.65	1285
MCM-41 (900 °C)	2.8	0.45	915

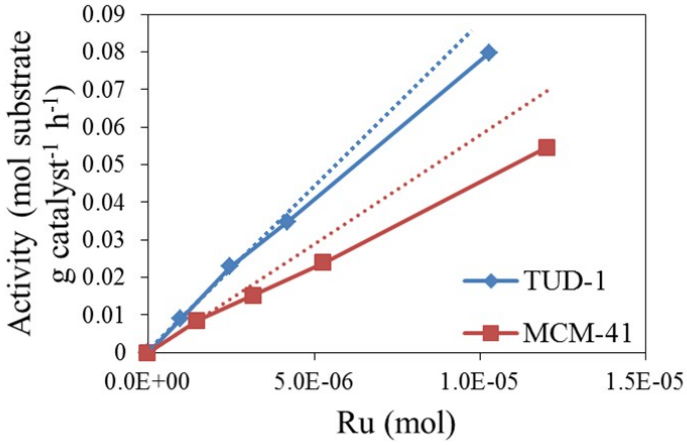

Figure S7. Initial activity of HG2/TUD-1 and HG2/MCM-41 with increasing loading of Ruthenium (mol). The dotted lines indicate the imagined linear increase in activity. The variation of the observed points indicates a deviation of this linear trend.

GPC analysis

Prior to GPC analysis, the reaction solvent was removed by evaporation to add THF instead. As a consequence, the more volatile cyclooctene is evaporated as well. Therefore the GPC signal of cyclooctene is not proportional to its real value. But since conversion of the reaction was determined by GC analysis, this does not form a problem. GPC was implemented to predict the product distributions. Higher (cyclic) oligomers (≥C16) were not prone to evaporation and could be compared with each other.

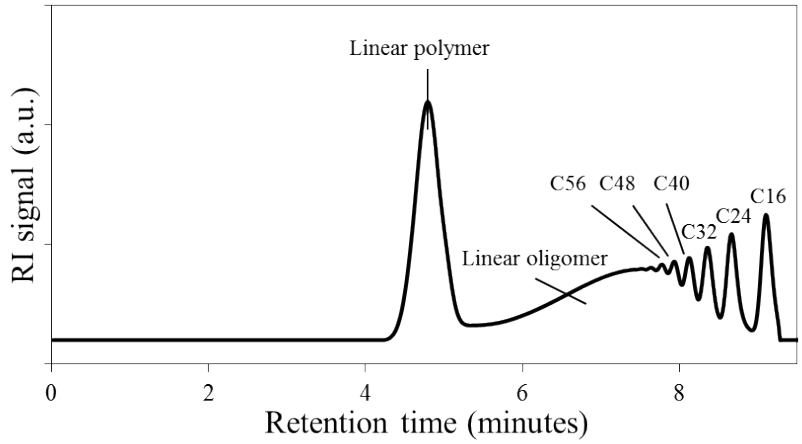

Figure S8. Example of a GPC chromatogram with specification of the different product fractions after metathesis of cyclooctene.

Kinetic dissimilarities of metathesis in porous silica

Modeling Ring-Chain Equilibria: Theory

A. Pioneers in modeling of ring-chain equilibria were Jacobson and Stockmayer, who developed a theory (**J-S theory**) hereof based on the following reaction equilibrium: $P_{i+j} \leftrightarrow P_j + C_i$; where P_{i+j} and P_j are linear polymers of degree of polymerization *i+j* and *j* respectively and C_i is a cyclic oligomer of degree of polymerization *i*. This theory includes the following assumptions: 1) All cyclic oligomers formed are free of ring-strain and ring-opening and ring-closing are entropically driven, 2) the probability of ring formation is governed by the fraction of all configurations for which the ends coincide, 3) the end-to-end distances of linear chains obey Gaussian statistics and 4) the reactivity of the chain ends is independent of chain length. Only an entropic term contributes to the equilibrium constant, and consists of a positive value due to the formation of two molecules from one and a negative value due to a decreased number of configurations when forming cyclic oligomers. The equilibrium constant (K_i) of this reaction depends therefore only on *i* (as entropy only reduces with increasing ring size *i* but is independent of *j*) and is given by:

$$K_i = \left(\frac{3}{2\pi < r_i^2 >_0}\right)^{3/2} \frac{1}{N_A \sigma_{R_i}}$$

where $<r_i^2>_0$ is the mean-squared end-to-end distance of a random chain of *i* units, N_A is Avogadro's number, σ_{Ri} is a symmetry number to eliminate over counting of indistinguishable configurations ($\sigma_{Ri} = 2i$ for cyclics).

Since $<r_i^2>_0 \infty i$, K_i the saturation concentration of a cyclic oligomer (C_i) with degree of polymerization *i* decreases with increasing ring size proportional to $i^{-5/2}$.

B. To correctly predict $\langle r_i^2 \rangle_0$ in order to obtain a realistic prediction of K_i, a rational isomeric static (RIS) model was used to correctly calculate the end-to-end distances of molecules. The resulted **JS-RIS model** is accurate for large cyclic oligomers, but not for smaller cycles as ring-strain is present and significantly affects ring-chain equilibrium.

C. Kornfield and co-workers further optimized this model and took into account ring-strain, the renewed equilibrium constants (K_i) being dependent on the enthalpy change and given by:

$$lnK_i = -\frac{\Delta H_i}{RT} + ln\left[\frac{1}{2iN_A}\left(\frac{3}{2\pi < r_i^2 >}\right)^{\frac{3}{2}}\right]$$

Modeling Ring-Chain Equilibria: Molar equilibrium constants

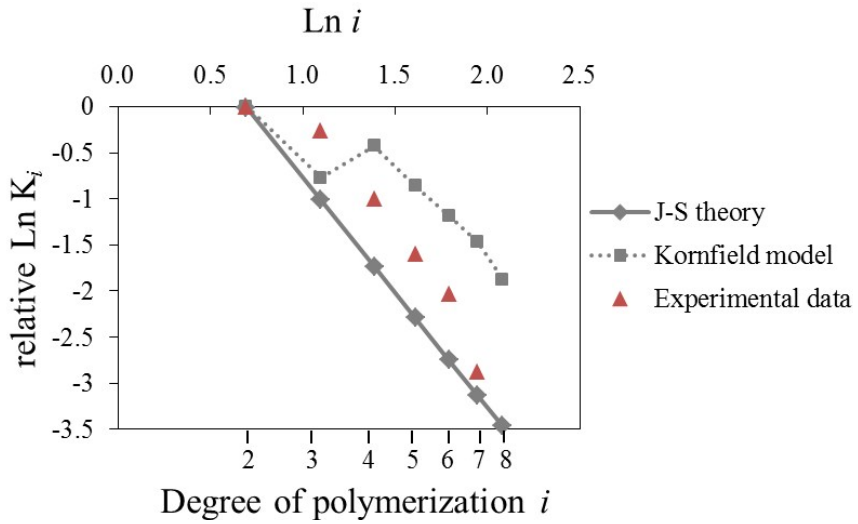

Figure S9. Plot of the relative ln K_i (molar equilibrium constant) vs. ln *i* (degree of polymerization *i*) for cyclic oligomers of cyclooctene. The molar equilibrium constants were compared between the J-S theory (full straight line with a slope of -5/2), an optimized model of ring-chain equilibria based on the J-S theory by Kornfield and coworkers (dotted line) and our experimental data (red dots). Concentration cyclooctene: 0.05 mol/L.

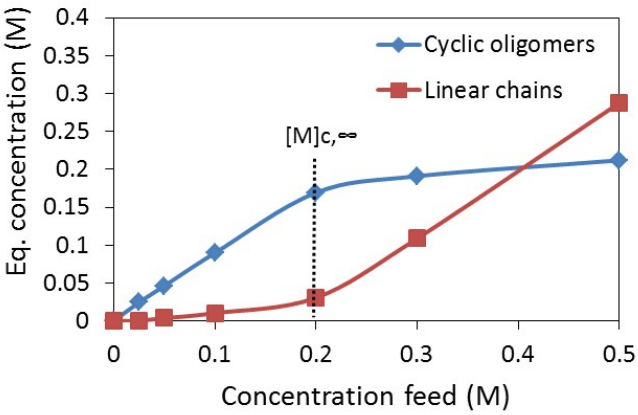

Figure S10. Equilibrium concentrations for cyclic oligomers and linear chains. The experimentally derived saturation concentration of cyclic oligomers approaches very well the theoretically determined critical monomer concentration of 0.21 mol/L.

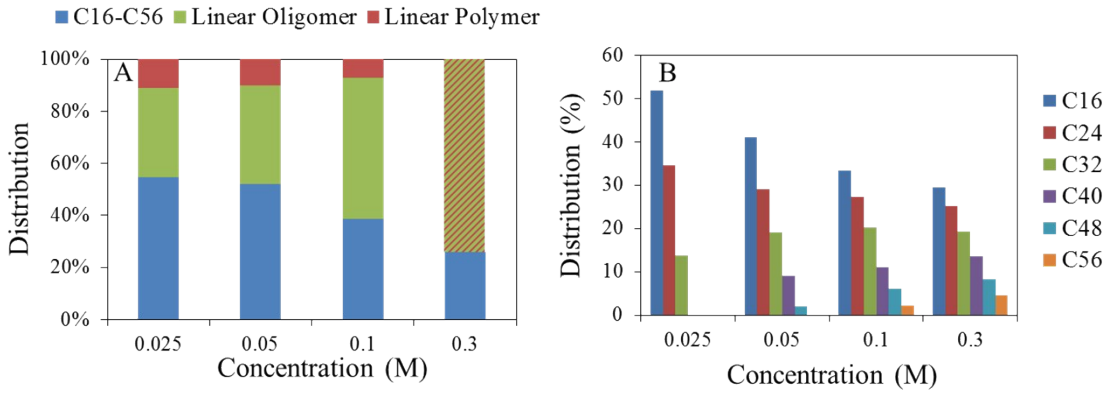

Figure S11. A) The effect of increasing monomer concentration on the product distribution (cyclic oligomers/linear oligomers/ linear polymers) at a cyclooctene conversion of 5 %. The linear fraction is summated at a concentration of 0.3 M due to presence of linear chains over a broad molecular weight range. B) Distribution (wt%) of C16-C56 cyclic oligomers at a cyclooctene conversion of 5 %. Reaction conditions: 0.025 – 0.3 M cyclooctene; 16 mL toluene, 3 mg HG2; 35 °C. The linear oligomer and polymer fraction were summated at 0.3 M due to difficult separation.

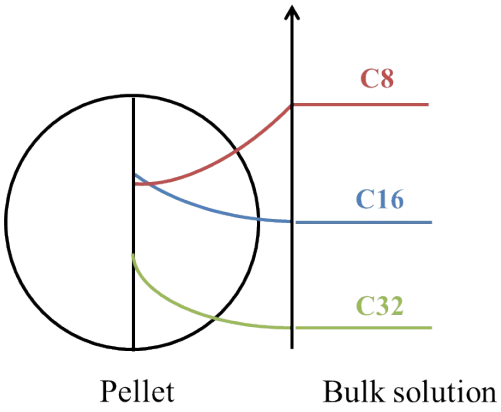

Figure S12. Schematic representation of the concentration of cyclooctene C8, the dimer C16 and the trimer C32 inside the pellet and in the bulk solution.

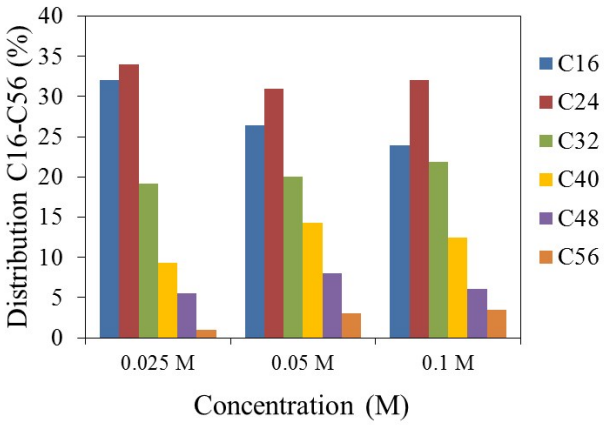

Figure S13. Distribution of C16-C56 cyclic oligomers at equilibrium with HG2/MCM-41 at different cyclooctene concentrations. Reaction conditions: 16 mL hexane; 160 mg HG2/MCM-41 (pretreated at 150 °C; 0.30 wt% Ru); 35 °C.

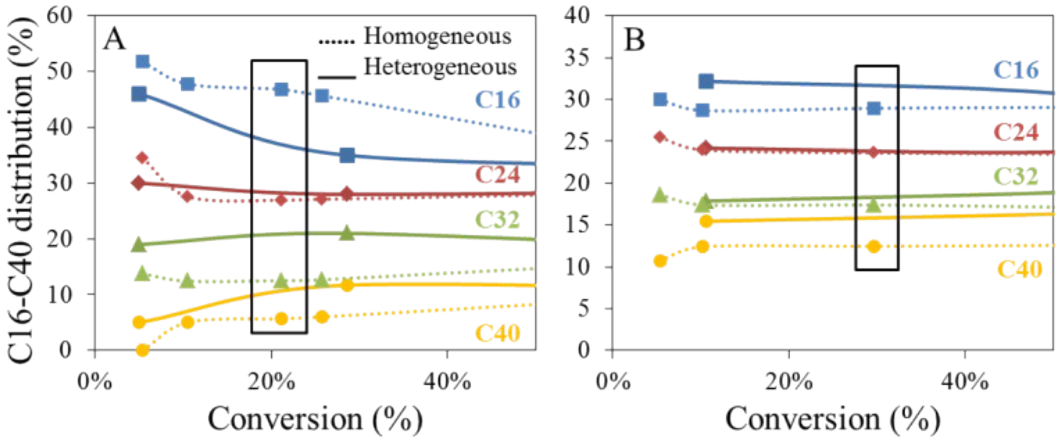

Figure S14. Distribution of C16-C40 cyclic oligomers for a homogeneous and heterogeneous catalyzed metathesis of cyclooctene at A)0.025 M and B) 0.1 M. Reaction conditions: 0.05 M cyclooctene; 16 mL toluene (homogeneous reaction) or hexane (heterogeneous reaction); 3 mg HG2 or 160 mg HG2/MCM-41 (pretreated at 150 °C; 0.30 wt% Ru); 35 °C.

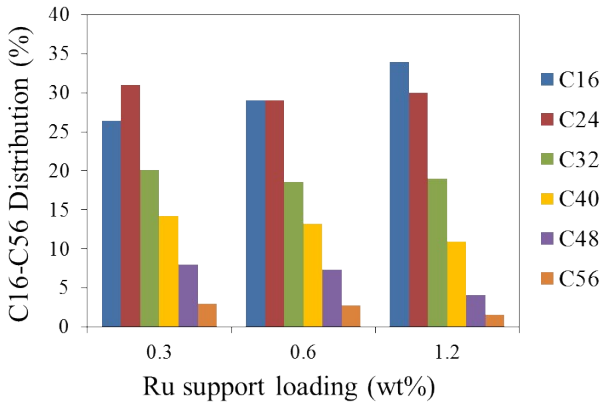

Figure S15. Distribution of C16-C56 cyclic oligomers (wt%) at increasing Ru loadings on MCM-41 at full cyclooctene conversion. Reaction conditions: 0.05 M cyclooctene; 16 mL hexane; 50 mg HG2/MCM-41 (pretreated at 150 °C), 35 °C.

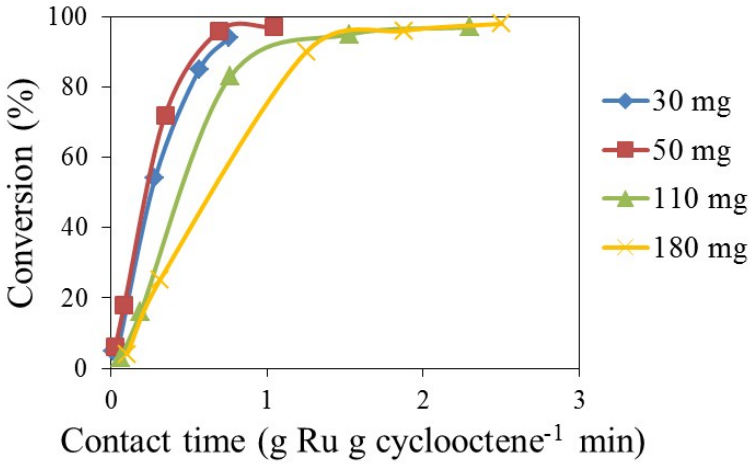

Figure S16. The effect of increasing the amount of catalyst (30-180 mg) on the conversion of cyclooctene. Reaction conditions: 0.05 M cyclooctene; 5 mL hexane; HG2/MCM-41 (pretreated at 150 °C; 0.29 wt%); 35 °C.

References

1. B. A. Morrow, I. A. Cody and L. S. M. Lee, *J. Phys. Chem.*, 1976, **80**, 2761-2767.
2. J.-P. Gallas, J.-M. Goupil, A. Vimont, J.-C. Lavalley, B. Gil, J.-P. Gilson and O. Miserque, *Langmuir*, 2009, **25**, 5825-5834.
3. B. A. Morrow and A. J. McFarlan, *The Journal of Physical Chemistry*, 1992, **96**, 1395-1400.
4. A. P. Legrand, *The Surface Properties of Silicas*, John Wiley & Sons, 1998.